Original Article

Carotid tortuosity is associated with extracranial carotid artery aneurysms

Constance J. H. C. M. van Laarhoven[1]^, Saskia I. Willemsen[1#]^, Jurre Klaassen[1,2#]^, Evelien E. de Vries[1], Quirine M. J. van der Vliet[3], Constantijn E. V. B. Hazenberg[1]^, Michiel L. Bots[4], Gert J. de Borst[1]^; Carotid Aneurysm Registry (CAR) study group*

[1]Department of Vascular Surgery, University Medical Center Utrecht, Utrecht University, Utrecht, The Netherlands; [2]Technical Medicine, University of Twente, Enschede, The Netherlands; [3]Department of Trauma Surgery, University Medical Center Utrecht, Utrecht University, Utrecht, The Netherlands; [4]Julius Center for Health Sciences and Primary Care, University Medical Center Utrecht, Utrecht University, Utrecht, The Netherlands

Contributions: (I) Conception and design: CJHCM van Laarhoven, GJ de Borst; (II) Administrative support: CJHCM van Laarhoven, GJ de Borst; (III) Provision of study materials or patients: CJHCM van Laarhoven, EE de Vries, QMJ van der Vliet, CEVB Hazenberg, GJ de Borst; (IV) Collection and assembly of data: CJHCM van Laarhoven, J Klaassen; (V) Data analysis and interpretation: CJHCM van Laarhoven, SI Willemsen, J Klaassen, ML Bots; (VI) Manuscript writing: All authors; (VII) Final approval of manuscript: All authors.

[#]These authors contributed equally to this work.

Correspondence to: Prof. Gert J. de Borst, MD, PhD. Department of Vascular Surgery, University Medical Center Utrecht, G04.129 PO Box 85500, 3508 GA Utrecht, The Netherlands. Email: g.j.deborst-2@umcutrecht.nl.

Background: Tortuous arteries may be associated with carotid dissection. The intima disruption caused by a carotid dissection is a possible cause of extracranial carotid artery aneurysms (ECAAs). The aim was to investigate if carotid tortuosity is also associated with ECAA in patients without presence or history of a carotid artery dissection.

Methods: A retrospective case-control study was performed including 35 unilateral ECAA patients (cases) and 105 age- and sex-matched controls. Tortuosity was expressed as tortuosity-index (TI), curvature, and torsion measured on computed tomography angiography (CTA) data in 3Mensio Vascular and MATLAB by two independent investigators. Primary comparison was tortuosity in ipsi- versus contralateral carotid artery within the cohort of ECAA patients. Secondary comparison was tortuosity with ipsilateral carotid arteries in control patients. All observations were assessed on inter- and intra-operator reproducibility.

^ ORCID: Constance J. H. C. M. van Laarhoven, 0000-0002-8817-7315; Saskia I. Willemsen, 0000-0003-0801-2439; Jurre Klaassen, 0000-0002-2490-5934; Constantijn E. V. B. Hazenberg, 0000-0002-2408-2720; Gert Jan de Borst, 0000-0002-1389-4141.

*Collaborator-Carotid Aneurysm Registry (CAR) study group: Martin Björck, Roberto Chiesa, Lazar Davidovic, Edit Dósa, Juha E Jaaskelainen, Antti Lindgren, Miroslav Markovic, Daniele Mascia, Joakim Nordanstig, Harue Santiago Kumakura, Erasmo Simão da Silva, Zoltán Szeberin. From the Department of Surgical Sciences (MB), Vascular Surgery, Uppsala University, Uppsala, Sweden; Division of Vascular Surgery (RC, DM), San Raffaele 'Vita-Salute' University, Ospedale San Raffaele, Milano, Italy; Clinic for Vascular and Endovascular Surgery (LD, MM), Faculty of Medicine, University of Belgrade, Clinical Centre of Serbia, Belgrade, Serbia; Department of Vascular and Endovascular Surgery (ZS), Heart and Vascular Center (ED), Hungarian Vascular Radiology Research Group (ED), Semmelweis University, Budapest, Hungary; Division of Neurosurgery (JJ, AL), Kuopio University Hospital, Kuopio, Finland; Department of Vascular Surgery and Institute of Medicine (JN), Department of Molecular and Clinical Medicine (JN), Sahlgrenska University Hospital and Academy, University of Gothenburg, Gothenburg, Sweden; Vascular and Endovascular Division (HSK, ESdS), Surgery Department, Hospital das Clinicas HCFMUSP, Faculdade de Medicina, Universidade de Sao Paulo, Sao Paulo, Brazil.

Results: Carotid tortuosity was comparable within the cohort of ECAA patients (Spearman correlation 0.76, P<0.001), yet distinctively higher in comparison with unilateral controls. After adjustment for patient characteristics, presence of ECAA was associated with TI (β 0.146, 95% CI: 0.100–0.192). All tortuosity observations showed excellent inter- and intra-operator reproducibility.

Conclusions: Carotid tortuosity seems to be a risk factor for development of ECAA. Surveillance of individuals with increased carotid tortuosity therefore potentially ensures prompt diagnosis and treatment of ECAA. However, future research should investigate if persons with an increased tortuosity do indeed develop ECAA.

Keywords: Tortuosity; extracranial carotid artery aneurysm (ECAA)

Submitted Feb 01, 2022. Accepted for publication Jul 19, 2022.
doi: 10.21037/qims-22-89
View this article at: https://dx.doi.org/10.21037/qims-22-89

Introduction

Extracranial carotid artery aneurysm (ECAA) is a rare vascular pathology (1,2). The clinical presentation and course are largely unknown but seem dependent on the etiology, carotid site, and size of the carotid aneurysm (2). Registry data from the ongoing international web-based Carotid Aneurysm Registry (CAR) (3) indicate that approximately one out of five patients presents with local symptoms (e.g., pulsatile mass), of which one sixth is affected by cerebral ischemia (stroke or transient ischemic attack). It has been suggested that tortuosity (such as sharp bends and kinks) in the course of the carotid artery may affect local hemodynamics, resulting in either dilated or stenotic lesions as a consequence (4-6). Moreover, tortuosity of the cervical arteries (both vertebral and carotid) has been suggested to be associated with arterial dissection, and in the carotid artery this intima disruption at its turn is a common cause of ECAA (1,7-9). Arterial tortuosity is commonly expressed as the tortuosity index (TI): the ratio of the length of curved, or central luminal line (CLL) of the artery and the straight line length between two anatomical landmarks (9-12). If carotid tortuosity is associated with carotid aneurysms without presence of arterial dissection, TI may be a candidate variable in future screening algorithms for ECAA and integration in prediction models for ECAA development. The objective of the present retrospective case-control study in patients without presence or history of carotid dissection, was to investigate if a high degree of carotid tortuosity is associated with ECAA. We present the following article in accordance with the STROBE reporting checklist (available at https://qims.amegroups.com/article/view/10.21037/qims-22-89/rc) (13).

Methods

Participants

Ethical approval for this study was provided by the Medical Research Ethics Committee of University Medical Center Utrecht (UMCU) on 5th December 2018 (No. 18-834), and the study was conducted according to the principles of the Declaration of Helsinki (as revised in 2013) and in accordance with the Dutch Medical Research Involving Human Subjects Act (WMO). A retrospective case-control study was conducted from single-center data from the UMCU included in the CAR (The registry protocol has been published previously) (3). Briefly, any patient aged 18-years or older diagnosed with an ECAA is included in this ongoing registry, independent of etiology or treatment strategy. Baseline characteristics and imaging follow-up data were collected in a prospective manner. Individual consent for this retrospective analysis was waived.

For the present study, a case was defined as a diagnosed ECAA patient included in the CAR. Cases were equally selected from the registry based on sex, age (younger and ≥55 years old), shape of aneurysm (fusiform or saccular), and both small (maximum diameter ≤10.0 mm) and large (>10.0 mm) ECAAs. The primary thin-slice (<1.0 mm) CTA of the carotids to confirm the ECAA diagnosis was used for this study. Age- and sex-matched controls were enrolled from subjects whom underwent a thin-slice CTA carotids as part of a trauma screening in the UMCU during the same study period. Cases and controls were matched in a ratio 1:3, with similar sex and age (range of 1 year). Both cases and controls were excluded and replaced if the arterial phase of the computed tomography angiography (CTA) was of poor

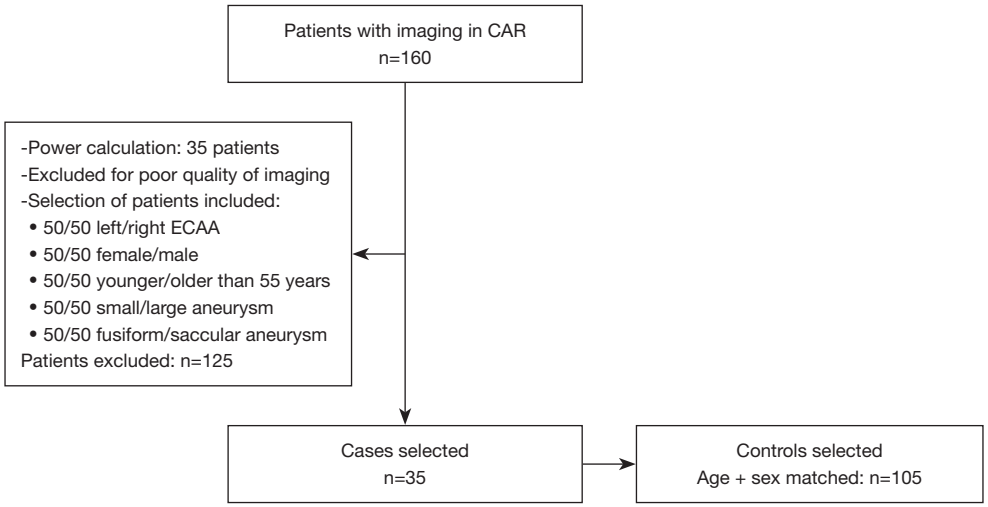

Figure 1 A flow diagram of the case and control selection. CAR, Carotid Aneurysm Registry; ECAA, extracranial carotid artery aneurysm.

quality. Additionally, cases were excluded in case of presence or history of carotid arterial dissection, mycotic, iatrogenic, dissecting, or bilateral ECAA. Controls were excluded in case of a trauma with direct impact on the neck region and/or a diagnosis of traumatic cervical artery dissection (*Figure 1*).

Clinical data

Vascular risk factors, including hypertension, diabetes mellitus, smoking, connective tissue disease (CTD), rheumatoid arthritis, and statin use of the cases were obtained from the CAR database. ECAA was defined as ≥150% fusiform dilatation of the carotid artery in comparison with the contralateral side, and saccular aneurysms of any size were accepted (14). Patient characteristics of the controls were obtained by patient chart review. The following definitions were used throughout the study: hypertension was defined as the use of any blood pressure lowering medication, or blood pressure >140/90 mmHg on repeated measurements. Diabetes was defined as usage of any blood glucose lowering medication. Current smoking was considered as tobacco usage within the last six months. CTD was defined as any genetically proven disorder, e.g., Marfan, Loeys-Dietz, or vascular Ehlers-Danlos syndromes. Rheumatoid arthritis was registered if diagnosed by a rheumatologist.

Imaging protocol

All CTA studies were performed using a 64- or 128-slice CT scanner (Philips Brilliance; Philips Medical Systems, Best, The Netherlands). Median slice thickness was 0.67 mm (range, 0.62–0.90 mm), increment 0.33, collimation 64×0.625 and pitch 1.2. Radiation exposure parameters were 100–120 kV and 150–300 mamp second. The field of view was set per patient. Injection of 65 mL intravascular contrast (Lopromide, Schering, Berlin, Germany) was followed by a saline bolus of 40 mL, both at a flow rate of 6.0 mL/s.

Imaging analysis

Every CTA scan was analyzed according to a pre-defined protocol with software of 3mensio Vascular (version 9.2, Pie Medical Imaging B.V., Maas tricht, the Netherlands). Using the vessel tool, a 3D image of the carotid arteries was generated. The central luminal line (CLL) of the carotid artery was automatically created and manually corrected. The carotid arteries were segmented in the curved planar reformation (CPR) of the vessel, measured from skull base to carotid bifurcation (internal carotid artery; ICA), and to the origin of the common carotid artery (CCA). The origin of the CCA was defined as the first slice in perpendicular plane in which the CCA was visible. The CLL length of the total carotid artery was calculated by adding lengths of ICA and CCA (*Figure 2*). The TI was measured on the CPR image as a ratio of the CLL length of the vessel to the straight line length between the two endpoints: TI = CLL length/Straight line length.

Additionally, coordinates of the 1.0 mm interpolated

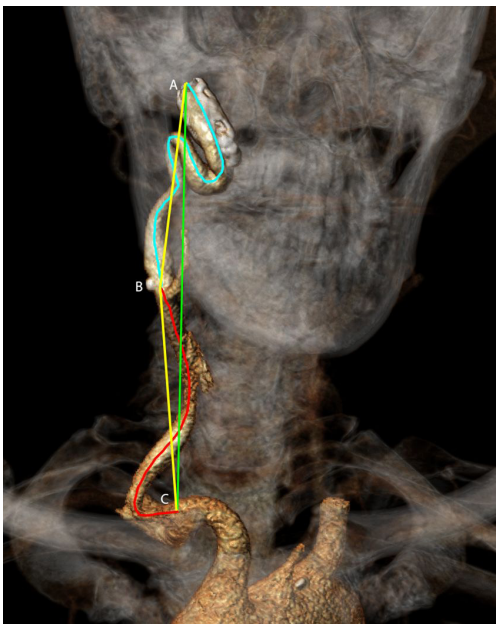

Figure 2 Segmentation example of the aneurysmal right ICA. The carotid tortuosity index was calculated for every study patient as ratio of the length of the CLL and the straight-line length. The carotid artery was measured from skull base (A) until carotid bifurcation (B), and origin of the CCA (C). The CLL for the ICA is indicated in blue, for the CCA in red. The CLL of the total carotid artery was calculated by adding ICA and CCA CLL length. The straight lines are indicated in yellow and green. ICA, internal carotid artery; CLL, central luminal line; CCA, common carotid artery.

CLL were exported from 3mensio Vascular, and analyzed with an in-house MATLAB (vR2019b, MathWorks®, Natick, Massachusetts, USA) based script to calculate the curvature and torsion of the total carotid artery. Applied equations for calculation of the extrinsic linear curvature and torsion are described in Appendix 1. Based on literature (4,5,15), the following cut-off values were applied; low (≤0.15), medium (>0.15 and ≤0.3), high (>0.3) curvature, and low (≤5.0), and high (>5.0) torsion values across the CLL of the entire carotid artery from CCA origin up to skull base. Total number of curvature and torsion categories per study subject were reported (*Figure 3*). All measurements were performed by two independent operators, of which the second was blinded for the outcomes of this study. Case or control status of the study subjects was blinded for both operators while measuring carotid tortuosity. To assess intra-operator variability, 35 scans (20%) were randomly selected and measured twice with a minimum wash-out period of 2 weeks. Both the operators were trained with five test patients, and the sequence of study patient measurements was determined by randomization to overcome a potential effect from learning.

Sample size calculation

The literature was reviewed for previous TI measurements of the extracranial carotid arteries for an accurate sample size calculation (8-10,12,16). For the healthy carotid artery, a mean TI of 1.2 was used, for the ECAA-affected carotid artery mean TI of 1.35, with standard deviation of 0.25. As a result, we obtained a sample size of 35 cases and 105 1:3 matched controls, 140 patients in total, one-sided with a power of 80% and type I error of 5%, calculated by use of the package '*epiR*' (17).

Outcome and statistical analysis

The primary parameter of interest was the difference of TI of the affected ipsilateral ECAA carotid artery compared with the contralateral artery within one ECAA patient, in order to correct for all confounding factors. The secondary parameter of interest was defined as the difference in TI in the affected carotid artery of ECAA patients compared with ipsilateral control carotids, adjusted for potential confounding factors. Additionally, number of curvature and torsion values of the carotid artery were analyzed in these groups. All observations were assessed in terms of inter- and intra-operator reliability and agreement. Reliability was assessed by use of Intraclass correlation coefficient (ICC; model: two-way mixed, type: absolute agreement) with 95% confidence intervals (CI). Bland-Altman analysis was used to assess agreement for TI (18,19). Normality was tested by the Shapiro-Wilk test. Non-parametrically distributed continuous and categorical baseline differences were compared with Mann Whitney U test, and χ^2 test respectively.

Carotid tortuosity within the ECAA patient

Continuous measures within one ECAA patient were compared by use of the paired *t*-test (parametrical), or Wilcoxon signed rank test (non-parametrical data). The correlations between continuous values were assessed with Pearson (parametrical) or Spearman correlation (non-parametrical data).

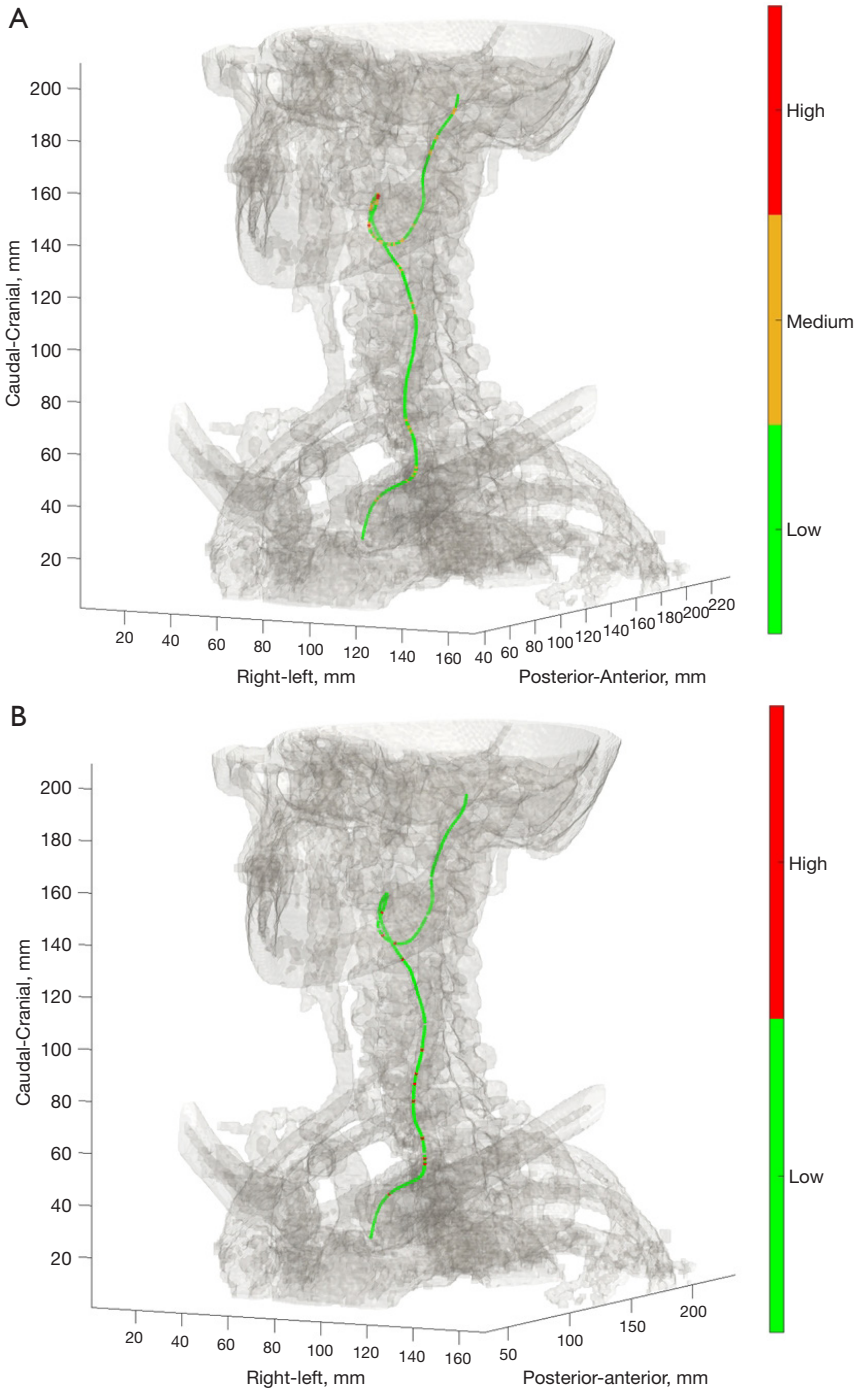

Figure 3 Example of curvature and torsion measures of the left carotid artery. The colored line represents the central luminal line of the total CA, left: curvature across the total CA divided in low (green; ≤0.15), medium (orange; >0.15 and ≤0.30), and high curvature (red; >0.30), right: torsion divided in low torsion (green; ≤5.0), and high torsion (red; >0.5). Applied equations are summarized in Appendix 1. CA, carotid artery.

Table 1 Baseline characteristics of study population

Variables	ECAA patients (n=35*)	Control patients (n=105)	P value
Male, n [%]	18 [51]	54 [51]	1
Age at scan, years, median [range]	62 [25–82]	62 [25–82]	0.983
Carotid side, n [%]			
Right	18 [51]	54 [51]	1
Hypertension, n [%]	16 [46]	34 [32]	0.179
Rheumatoid arthritis, n [%]	3 [9]	6 [6]	0.688
Diabetes mellitus, n [%]	3 [9]	7 [7]	0.706
Connective tissue disorder, n [%]	2 [6]	0	0.058
Statin use, n [%]	14 [40]	27 [26]	0.133
Smoking, n [%]	4 [11]	15 [14]	0.782

*, for one case no medical history was available. ECAA, extracranial carotid artery aneurysm.

Carotid tortuosity compared in ECAA patients and controls

Cases and controls were compared by use of the independent *t*-test, or Mann-Whitney U-test. Multiple linear regression analysis was used to correct for confounding. Potential confounders were selected based on a univariate analysis (P<0.1) and literature (5,7,9,12,20-22). Regression coefficients with 95% CI were reported, and P values <0.05 were considered statistically significant. The distribution of the residuals was checked with a Q-Q plot. All statistical analyses were conducted using SPSS v25.0 (IBM SPSS Statistics for Windows, Version 25.0. Armonk, NY: IBM Corp.) and Rstudio v3.4.1 (RStudio Team (2016). RStudio: Integrated Development for R. RStudio, Inc., Boston, MA, www.rstudio.com).

Results

From the CAR database, 35 unilateral ECAA cases were selected based on sex, age, shape and size of the ECAA. Thus, patients with bilateral ECAA were excluded. Out of >3,000 trauma patients, 105 eligible control patients, matched for age and sex, were included. Baseline characteristics of the separate patient groups are summarized in *Table 1*. Half of the patients (51%) were men with a median age of 62 years (range, 25–82 years). No statistically significant differences in cases and controls were observed in terms of cardiovascular medical history. CTD was seen in 2 patients (6%, P=0.058) in the case group, against no CTD patients in the control group. However, no statistically significant difference was seen which might be due to the small number of cases. Reported maximum diameters of either saccular or fusiform ECAAs were median 13.5 mm (range, 4.5–40.5 mm).

Inter- and intra-operator reproducibility

In total, 175 TI measurements were performed in 140 unique subjects (35 ECAA cases, 35 contralateral ECAA controls and 105 control trauma patients). The TI measurements were performed on the ICA, the CCA and the total CA. Excellent inter- and intra-operator reliability was observed with ICCs ≥0.9 (Table S1). Bland-Altman plots showed no systematic bias and limits of agreement were exceeded by less than 10% of the total dataset indicating normal differences (Figures S1,S2). No difference was seen in the TI measurements observed by the operator blinded for the outcomes and the operator not blinded for outcomes (data not shown).

Carotid tortuosity within the ECAA patient

Measures of TI, curvature and torsion of the different subfields of the carotid arteries of included ECAA patients are shown in *Table 2*. No distinctive differences in the unilateral ECAA artery and contralateral non-affected extracranial carotid artery in any of the subfields (ICA, CCA, or total CA) were seen. The highest TIs overall were observed in the ICA. Medium and high curvature numbers were rare across both carotids, indicating similar counts of

Table 2 Tortuosity measures in cases, compared with own contralateral carotid artery

Tortuosity index	Ipsilateral ECAA carotid artery, median (range) (n=35)	Contralateral carotid artery, median (range) (n=34*)	P value
ICA			
Overall	1.387 (1.066–2.145)	1.346 (1.022–2.028)	0.369
Left carotid	1.398 (1.072–1.840)	1.357 (1.022–1.681)	0.163
Right carotid	1.335 (1.066–2.145)	1.287 (1.026–2.028)	0.795
CCA			
Overall	1.108 (1.016–1.694)	1.089 (1.010–1.864)	0.573
Left carotid	1.108 (1.021–1.424)	1.084 (1.014–1.406)	0.055
Right carotid	1.105 (1.016–1.694)	1.143 (1.010–1.864)	0.344
Total CA			
Overall	1.245 (1.046–1.793)	1.229 (1.023–1.943)	0.726
Left carotid	1.249 (1.046–1.553)	1.227 (1.023–1.491)	0.381
Right carotid	1.241 (1.080–1.793)	1.233 (1.028–1.943)	0.586
Curvature (counts)**			
Low (≤0.15)	186 (147–230)	195 (148–240)	0.565
Medium (0.16–0.30)	40 (23–60)	39 (5–360)	0.280
High (>0.30)	5 (0–15)	5 (0–20)	0.312
Torsion (counts)**			
Low (≤5.0)	227 (177–525)	229 (177–259)	0.627
High (>5.0)	7 (1–13)	7 (1–16)	0.599

*, one patient with contralateral occlusion; **, only 33 *vs*. 30 segmentations available for curvature and torsion calculation across total CA. ECAA, extracranial carotid artery aneurysm; ICA, internal carotid artery; CCA, common carotid artery; CA, carotid artery.

sharp bends in both carotids. Lastly, nearly similar numbers of torsion were observed. Spearman correlation between the ipsi- and contralateral TI of the total carotid artery was 0.758 (P<0.001).

Carotid tortuosity compared in ECAA patients and controls

Significant differences in TI were observed when comparing the ECAA affected extracranial carotid artery with unilateral controls (*Table 3*). This difference remained intact when using the Bonferroni correction (α=0.00357). Furthermore, TI was higher in the ICA than CCA or total carotid artery. Both medium and high curvature counts across the total CA were higher within cases compared to controls (P<0.001). In contrast, for high torsion counts, no differences were observed.

Multiple linear regression was performed on TI measures of total carotid artery in unilateral cases and controls. Covariates were age ≥65 years, sex, carotid side, hypertension, CTD, and lastly presence of ECAA. Presence of ECAA (B 0.146, 95% CI: 0.100–0.192, P<0.001) was independently associated with an increased TI. The multiple linear regression can be seen in *Table 4*. The residuals followed a normal distribution.

Discussion

The present retrospective case-control study showed that carotid tortuosity is similar in the affected ipsi- versus non-affected contralateral carotid artery within ECAA patients, but distinctively higher in comparison with control patients. The difference in tortuosity between cases and controls remained significant after adjustment for potential confounding factors. Excellent inter- and intra-operator

Table 3 Tortuosity measures of cases and sex- and age-matched controls (unadjusted for confounding)

Tortuosity index	Ipsilateral ECAA carotid artery, median (range) (n=35)	Control carotid artery, median (range) (n=105)	P value
ICA			
Overall	1.387 (1.066–2.145)	1.122 (1.009–2.048)	<0.001
Left carotid	1.398 (1.072–1.840)	1.150 (1.017–2.048)	<0.001
Right carotid	1.335 (1.066–2.145)	1.112 (1.009–1.641)	<0.001
CCA			
Overall	1.108 (1.016–1.694)	1.051 (1.008–1.373)	0.010
Left carotid	1.108 (1.021–1.424)	1.050 (1.008–1.287)	0.029
Right carotid	1.105 (1.016–1.694)	1.056 (1.010–1.373)	0.182
Total CA			
Overall	1.245 (1.046–1.793)	1.105 (1.018–1.570)	<0.001
Left carotid	1.249 (1.046–1.553)	1.109 (1.021–1.570)	<0.001
Right carotid	1.241 (1.080–1.793)	1.103 (1.018–1.501)	<0.001
Curvature (counts)*			
Low (≤0.15)	186 (147–230)	189 (139–234)	0.716
Medium (0.16–0.30)	40 (23–60)	24 (2–52)	<0.001
High (>0.30)	5 (0–15)	0 (0–11)	<0.001
Torsion (counts)*			
Low (≤5.0)	227 (177–525)	200 (159–252)	<0.001
High (>5.0)	7 (1–13)	6 (2–12)	0.203

*, Only 33 vs. 92 segmentations available for curvature and torsion calculation across total CA. ECAA, extracranial carotid artery aneurysm; ICA, internal carotid artery; CCA, common carotid artery; CA, carotid artery.

Table 4 Multiple linear regression

Variables	B	95% CI	P value	t-value
Presence of ECAA	0.146	0.100 to 0.192	<0.001	6.327
Age, older than 65 years	0.071	0.031 to 0.111	0.001	3.506
Aneurysm side, right	0.018	–0.020 to 0.56	0.347	0.944
Female gender	0.033	0.072 to 0.005	0.087	1.722
CTD	–0.079	–0.244 to 0.085	0.342	–0.953
Hypertension	0.032	–0.009 to 0.074	0.127	1.535

B, unstandardized coefficient B; ECAA, extracranial carotid artery aneurysm; CTD, connective tissue disease.

reproducibility was observed in all TI measurements.

Arterial tortuosity is a commonly observed, though its pathological and clinical relevance are still under debate. Both TI (9,21) and curvature (5,15,21) of the carotids were investigated in patients with intracranial aneurysms, and even though the methods used to assess tortuosity varied, associations of high tortuosity with aneurysm formation were reported. The finding that arterial bends affect hemodynamic forces was confirmed by several computational hemodynamic studies (5,15,23). Fluctuating

wall shear stresses caused slow flow within aneurysms, and areas with highest curvature were prone to aneurysm formation (4,15,23). The present study confirms the association of high arterial tortuosity, defined as a high TI, and the presence of aneurysm in the extracranial carotid artery. Available literature reports that most ECAAs are located within the ICA (24-26), and in this subfield the highest values of TI were measured (*Tables 2,3*). This study shows that carotid tortuosity is a non-invasive measure easily calculated from standard imaging CT protocols and is therefore a promising candidate variable in radiological characterization of ECAA. At this point, optimal treatment and follow-up of ECAAs, or patients with increased tortuosity of the carotid arteries, is largely unknown (2,27). The European Society for Vascular Surgery (ESVS) clinical Guidelines on carotid and vertebral artery disease do not include recommendations on ECAAs, nor on surveillance of patients with tortuous ICAs (28).

Invasive endovascular or surgical treatment seems to be indicated in ECAA patients with symptoms and/or growing aneurysms (27). Even though open surgery remains the gold standard for these patients, significant comorbidities as a cranial nerve deficit should be considered. Endovascular repair should also be considered in poorly accessible distal aneurysms and hostile necks (29). The effect of carotid tortuosity and its potential to hamper endovascular treatment options of ECAA remains to be investigated. In a recent study higher TI was associated with occlusion after endovascular repair of popliteal aneurysms (30). Also, previous research on patients with thoracic aneurysms treated with Thoracic Endovascular Aneurysm Repair (TEVAR) showed impressive stent displacement forces in patients with thoracic tortuosity (31). Even though the blood pressure is likely to differ within the carotids, the tortuous anatomy could mimic displacement forces after carotid stenting and cause migration of the stent. Defining a future quantitative tortuosity threshold for endovascular therapy, will aid in selecting eligible patients for endovascular stenting of ECAA.

Although our study was powered on the difference in TI for case and control patients, we have additionally analyzed the ipsi- and contralateral artery within ECAA patients, in contrast to other studies (5,21,32). Confounding factors for tortuosity were corrected for in this analysis. The affected ECAA carotid artery showed overall higher numerical TI values than the contralateral side, but no significant differences were observed, neither in curvature nor in torsion values (*Table 2*). This may be a result of type-II statistical error, however, since only 35 patients with ECAA were studied. Similar bilateral TI was also observed in a sample of unilateral extracranial artery dissection patients (9). In this study, it was suggested that the side of the dissection might be determined by the side of injury. However, this could not be further investigated. Nevertheless, the exact moment of development of both dissection and ECAA is difficult to pinpoint. The time difference between de the development and detection of the ECAA will therefore remain unknown. Future longitudinal research is warranted to overcome antecedent-consequent bias and should focus on whether the contralateral side develops ECAAs in time as well. Bilateral tortuosity may indicate that these patients have a generalized tortuous vascular subtype, such as the monogenetic disease "arterial tortuosity syndrome" (33), although it remains unclear if this predisposes for bilateral ECAA disease. It is possible that arterial tortuosity could be used as surrogate marker of a vascular subtype, prone to aneurysm formation. Furthermore, it is imaginable that ECAAs with large diameters affect the carotid geometry more, and growth of the aneurysm sac could potentially affect future endovascular options. As the present study was not powered on the difference in tortuosity for aneurysm size, stratification into large (>10 mm) and small (≤10 mm) ECAA did not influence the results within the ECAA patient (P>0.338, data not shown). Our study results can be used as baseline values for future research to investigate the difference in arterial tortuosity stratified in ECAA size. Besides age (7,12,20) and aneurysm presence (5,21,34), male sex, hypertension (22), and CTDs (35) were suggested to be associated with tortuosity. In the present analysis, these findings for age and aneurysm presence were confirmed.

Limitations

Selection of a dissection-free study sample is challenging. Arterial dissection may be asymptomatic, and radiological identification of the characteristic intima flap or mural hematoma is hampered by time-dependent vascular remodeling. The potential influence of dissection on carotid tortuosity and ECAA, is therefore not a potential residual confounder. Secondly, assessment of curvature and torsion have been rarely investigated for the extracranial carotid arteries. In order to report our results accessibly, we defined cut-off values according to the existing literature (4,5,15) to indicate degree of curvature and torsion (*Figure 2*). Suitable thresholds and their clinical applicability remain

to be investigated. In addition, curvature and torsion values were solely available for the total CLL and thus the entire carotid artery. Further optimization of software should be performed to enable discrimination and assess curvature and torsion in the ICA and CCA separately. As in every medical imaging derived study, the present results are highly dependent on the quality of the scan. Deviating head- and neck-postures while scanning could influence carotid geometry, in particular the length of the straight line of the carotid artery. Since we observed angulation in only a few subjects, both cases and controls, we consider this influence negligible. Lastly, manual correction of the automatically generated CLL by the 3mensio Vascular software was necessary in every study subject causing potential variability of the results. Despite these manual corrections, reproducibility of the present tortuosity measures between operators was excellent mainly due to our detailed pre-defined scoring protocol. Quantitative 3D tortuosity measures by use of well-defined protocols are therefore the recommended first step in future research on tortuosity. Ultimately, fully automatic TI measurements can be computed by machine learning and could be integrated in future screening algorithms for ECAA (36).

Conclusions

This retrospective case-control study showed that carotid tortuosity is similar in both carotids within ECAA patients, though significantly higher in comparison with age- and sex-matched controls. Carotid tortuosity therefore seems to be associated with ECAA development. Future research should investigate if persons with an increased tortuosity do indeed develop ECAA and would benefit from surveillance of their carotid arteries.

Acknowledgments

Funding: None.

Footnote

Reporting Checklist: The authors have completed the STROBE reporting checklist. Available at https://qims.amegroups.com/article/view/10.21037/qims-22-89/rc

Conflicts of Interest: All authors have completed the ICMJE uniform disclosure form (available at https://qims.amegroups.com/article/view/10.21037/qims-22-89/coif). The authors have no conflicts of interest to declare.

Ethical Statement: The authors are accountable for all aspects of the work in ensuring that questions related to the accuracy or integrity of any part of the work are appropriately investigated and resolved. The study was conducted in accordance with the Declaration of Helsinki (as revised in 2013) and the Dutch Medical Research Involving Human Subjects Act (WMO). The study was approved by Medical Research Ethics Committee of the University Medical Center Utrecht (UMCU) on 5th December 2018 (No. 18-834) and individual consent for this retrospective analysis was waived.

References

1. Welleweerd JC, Nelissen BG, Koole D, de Vries JP, Moll FL, Pasterkamp G, Vink A, de Borst GJ. Histological analysis of extracranial carotid artery aneurysms. PLoS One 2015;10:e0117915.
2. Welleweerd JC, den Ruijter HM, Nelissen BG, Bots ML, Kappelle LJ, Rinkel GJ, Moll FL, de Borst GJ. Management of extracranial carotid artery aneurysm. Eur J Vasc Endovasc Surg 2015;50:141-7.
3. Welleweerd JC, Bots ML, Kappelle LJ, Rinkel GJ, Ruigrok YM, Baas AF, van der Worp HB, Vergouwen MD, Bleys RL, Hendrikse J, Lo TR, Moll FL, de Borst GJ. Rationale and design of the extracranial Carotid artery Aneurysm Registry (CAR). J Cardiovasc Surg (Torino) 2018;59:692-8.
4. Dolan JM, Kolega J, Meng H. High wall shear stress and spatial gradients in vascular pathology: a review. Ann Biomed Eng 2013;41:1411-27.
5. Lauric A, Safain MG, Hippelheuser J, Malek AM. High curvature of the internal carotid artery is associated with the presence of intracranial aneurysms. J Neurointerv Surg 2014;6:733-9.
6. Norman PE, Powell JT. Site specificity of aneurysmal

disease. Circulation 2010;121:560-8.
7. Saba L, Argiolas GM, Sumer S, Siotto P, Raz E, Sanfilippo R, Montisci R, Piga M, Wintermark M. Association between internal carotid artery dissection and arterial tortuosity. Neuroradiology 2015;57:149-53.
8. Giossi A, Mardighian D, Caria F, Poli L, De Giuli V, Costa P, Morotti A, Gamba M, Gilberti N, Ritelli M, Colombi M, Sessa M, Grassi M, Padovani A, Gasparotti R, Pezzini A. Arterial tortuosity in patients with spontaneous cervical artery dissection. Neuroradiology 2017;59:571-5.
9. Kim BJ, Yang E, Kim NY, Kim MJ, Kang DW, Kwon SU, Kim JS. Vascular Tortuosity May Be Associated With Cervical Artery Dissection. Stroke 2016;47:2548-52.
10. de Vries EE, Pourier VEC, van Laarhoven CJHCM, Vonken EJ, van Herwaarden JA, de Borst GJ. Comparability of semiautomatic tortuosity measurements in the carotid artery. Neuroradiology 2019;61:147-53.
11. Chen CK, Chou HP, Guo CY, Chang HT, Chang YY, Chen IM, Wu MH, Shih CC. Interobserver and intraobserver variability in measuring the tortuosity of the thoracic aorta on computed tomography. J Vasc Surg 2018;68:1183-1192.e1.
12. Choudhry FA, Grantham JT, Rai AT, Hogg JP. Vascular geometry of the extracranial carotid arteries: an analysis of length, diameter, and tortuosity. J Neurointerv Surg 2016;8:536-40.
13. Sharp SJ, Poulaliou M, Thompson SG, White IR, Wood AM. A review of published analyses of case-cohort studies and recommendations for future reporting. PLoS One 2014;9:e101176.
14. Pourier VEC, Welleweerd JC, Kappelle LJ, Rinkel GJE, Ruigrok YM, van der Worp HB, Lo TH, Bots ML, Moll FL, de Borst GJ. Experience of a single center in the conservative approach of 20 consecutive cases of asymptomatic extracranial carotid artery aneurysms. Eur J Neurol 2018;25:1285-9.
15. Lauric A, Hippelheuser J, Safain MG, Malek AM. Curvature effect on hemodynamic conditions at the inner bend of the carotid siphon and its relation to aneurysm formation. J Biomech 2014;47:3018-27.
16. McNamara JR, Fulton GJ, Manning BJ. Three-dimensional computed tomographic reconstruction of the carotid artery: identifying high bifurcation. Eur J Vasc Endovasc Surg 2015;49:147-53.
17. Nunes T, Heuer C, Marshall J, Sanchez J, Thornton R, Reiczigel J, et al. Package ' epiR.' 2018. Available online: https://cran.r-project.org/package=epiR
18. de Vet HC, Terwee CB, Knol DL, Bouter LM. When to use agreement versus reliability measures. J Clin Epidemiol 2006;59:1033-9.
19. Kottner J, Audigé L, Brorson S, Donner A, Gajewski BJ, Hróbjartsson A, Roberts C, Shoukri M, Streiner DL. Guidelines for Reporting Reliability and Agreement Studies (GRRAS) were proposed. J Clin Epidemiol 2011;64:96-106.
20. Tawfik AM, Sobh DM, Gadelhak B, Sobh HM, Batouty NM. The effect of age and gender on tortuosity of the descending thoracic Aorta. Eur J Radiol 2019;110:54-9.
21. Kliś KM, Krzyżewski RM, Kwinta BM, Stachura K, Gąsowski J. Tortuosity of the Internal Carotid Artery and Its Clinical Significance in the Development of Aneurysms. J Clin Med 2019;8:237.
22. Zenteno M, Viñuela F, Moscote-Salazar LR, Alvis-Miranda H, Zavaleta R, Flores A, et al. Clinical implications of internal carotid artery tortuosity, kinking and coiling: a systematic review. Rom Neurosurg 2014;21:51-60.
23. Lee AY, Sanyal A, Xiao Y, Shadfan R, Han HC. Mechanical instability of normal and aneurysmal arteries. J Biomech 2014;47:3868-75.
24. Martins de Souza N, Vikatmaa P, Tulamo R, Venermo M. Etiology and treatment patterns of ruptured extracranial carotid artery aneurysm. J Vasc Surg 2021;74:2097-2103.e7.
25. Nordanstig J, Gelin J, Jensen N, Osterberg K, Strömberg S. National experience with extracranial carotid artery aneurysms: epidemiology, surgical treatment strategy, and treatment outcome. Ann Vasc Surg 2014;28:882-6.
26. van Laarhoven CJHCM, Pourier VEC, Lindgren AE, Vergouwen MDI, Jääskeläinen JE, Rinkel GJE, de Kleijn DPV, de Borst GJ. Co-prevalence of extracranial carotid aneurysms differs between European intracranial aneurysm cohorts. PLoS One 2020;15:e0228041.
27. Pourier VE, De Borst GJ. Which carotid artery aneurysms need to be treated (and how)? J Cardiovasc Surg (Torino) 2016;57:152-7.
28. Naylor AR, Ricco JB, de Borst GJ, Debus S, de Haro J, Halliday A, et al. Editor's Choice - Management of Atherosclerotic Carotid and Vertebral Artery Disease: 2017 Clinical Practice Guidelines of the European Society for Vascular Surgery (ESVS). Eur J Vasc Endovasc Surg 2018;55:3-81.
29. Li Z, Chang G, Yao C, Guo L, Liu Y, Wang M, Liu D, Wang S. Endovascular stenting of extracranial carotid artery aneurysm: a systematic review. Eur J Vasc Endovasc Surg 2011;42:419-26.
30. Cervin A, Acosta S, Hultgren R, Grip O, Björck M, Falkenberg M. Results After Open and Endovascular

Repair of Popliteal Aneurysm: A Matched Comparison Within a Population Based Cohort. Eur J Vasc Endovasc Surg 2021;61:988-97.
31. Belvroy VM, Romarowski RM, van Bakel TMJ, van Herwaarden JA, Bismuth J, Auricchio F, Moll FL, Trimarchi S. Impact of Aortic Tortuosity on Displacement Forces in Descending Thoracic Aortic Aneurysms. Eur J Vasc Endovasc Surg 2020;59:557-64.
32. Labeyrie PE, Braud F, Gakuba C, Gaberel T, Orset C, Goulay R, Emery E, Courthéoux P, Touzé E. Cervical artery tortuosity is associated with intracranial aneurysm. Int J Stroke 2017;12:549-52.
33. Beyens A, Albuisson J, Boel A, Al-Essa M, Al-Manea W, Bonnet D, et al. Arterial tortuosity syndrome: 40 new families and literature review. Genet Med 2018;20:1236-45.
34. Kim BJ, Lee SH, Kwun BD, Kang HG, Hong KS, Kang DW, Kim JS, Kwon SU. Intracranial Aneurysm Is Associated with High Intracranial Artery Tortuosity. World Neurosurg 2018;112:e876-80.
35. Welby JP, Kim ST, Carr CM, Lehman VT, Rydberg CH, Wald JT, Luetmer PH, Nasr DM, Brinjikji W. Carotid Artery Tortuosity Is Associated with Connective Tissue Diseases. AJNR Am J Neuroradiol 2019;40:1738-43.
36. Katsuki M, Kakizawa Y, Nishikawa A, Yamamoto Y, Uchiyama T. Easily created prediction model using deep learning software (Prediction One, Sony Network Communications Inc.) for subarachnoid hemorrhage outcomes from small dataset at admission. Surg Neurol Int 2020;11:374.

Cite this article as: van Laarhoven CJHCM, Willemsen SI, Klaassen J, de Vries EE, van der Vliet QMJ, Hazenberg CEVB, Bots ML, de Borst GJ; Carotid Aneurysm Registry (CAR) study group. Carotid tortuosity is associated with extracranial carotid artery aneurysms. Quant Imaging Med Surg 2022;12(11):5018-5029. doi:10.21037/qims-22-89

Appendix 1

For calculation of the curvature of the central luminal line (CLL) of the carotid artery, the following equation of the extrinsic linear curvature was used (18):

$$\kappa = \frac{\sqrt{(z''y' - y''z')^2 + (x''z' - z''x')^2 + (y''x' - x''y')^2}}{(x'2 + y'2 + z'2)^{(3/2)}} \quad [1]$$

To calculate torsion of the CLL, the following equation derived from the theory described by Pressley (19) was used:

$$\tau = \frac{(x'''(y'z'' - y''z') + y'''(x''z' - x'z'') + z'''(x'y'' - x''y'))}{((y'z'' - y''z')^2 + (x^\wedge z' - x'z'')^2 + (x'y'' - x''y')^2)} \quad [2]$$

Where x,y,z are the CLL cartesian coordinates, ' is the first derivative, '' is the second derivative and ''' is the third derivative.

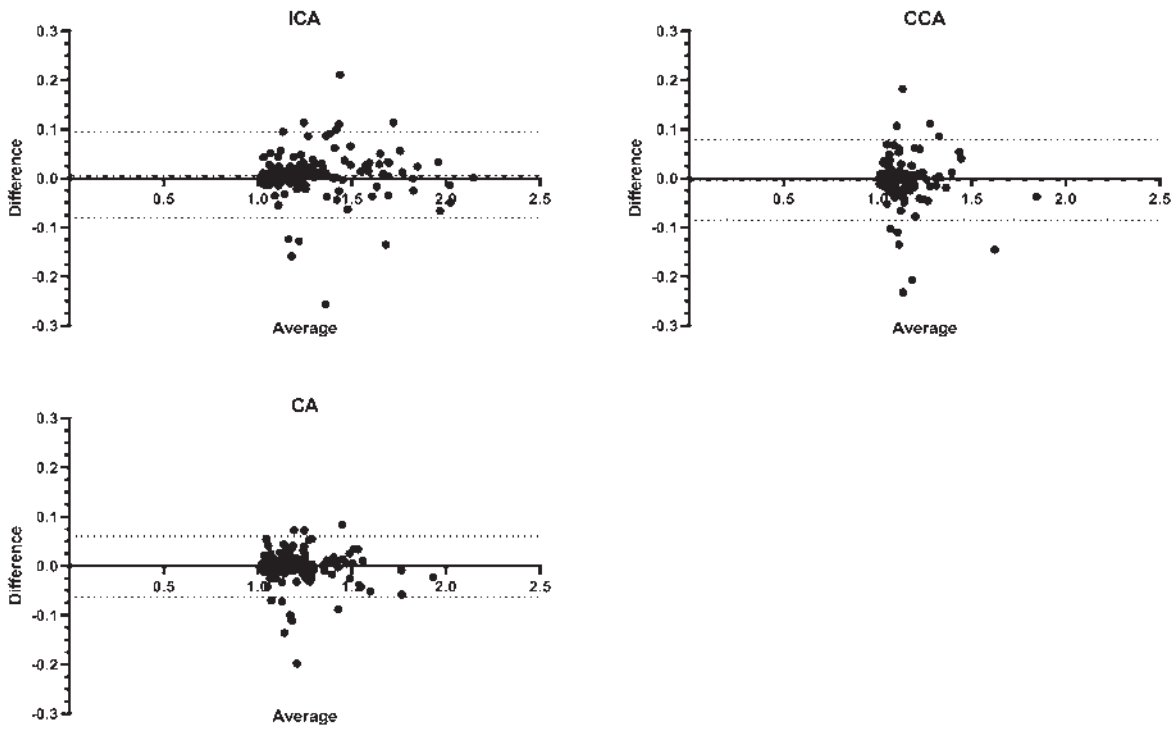

Figure S1 Bland-Altman plots showing agreement of two operators on tortuosity index (TI) measurements of 175 carotids according to the three subfields [internal carotid artery (ICA), common carotid artery (CCA), total carotid artery (CA)]. The dash-dotted line in the middle represents the mean difference of the TI between the two operators, and the dotted lines represent the upper and lower limits of agreement (mean difference ± 1.96 × standard deviation).

https://dx.doi.org/10.21037/qims-22-89

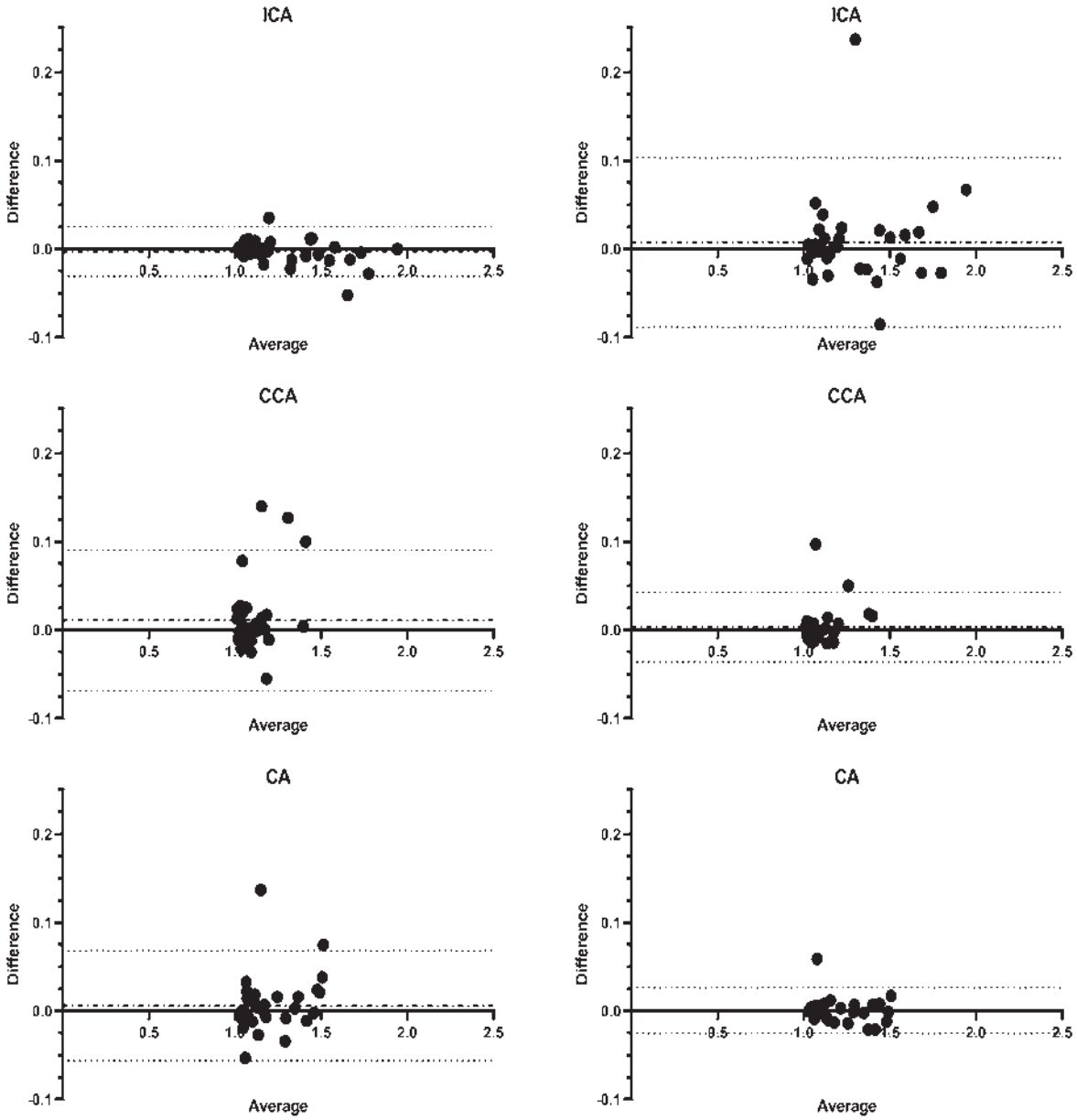

Figure S2 Bland-Altman (18,19) plots showing intra-operator agreement of operator 1 (blinded) in the left panel, and operator 2 on the right on tortuosity index (TI) measurements of 35 carotids according to the three subfields [internal carotid artery (ICA), common carotid artery (CCA), total carotid artery (CA)]. The dash-dotted line in the middle represents the mean difference of the TI between the two operators, and the dotted lines represent the upper and lower limits of agreement (mean difference ± 1.96 × standard deviation).

https://dx.doi.org/10.21037/qims-22-89

Table S1 Intraclass correlation coefficients for both inter- and intra-operator reliability (18,19)

	Inter-operator (n=175)		Intra-operator (n=35)			
			Operator 1*		Operator 2	
	ICC	(95% CI)	ICC	(95% CI)	ICC	(95% CI)
ICA	0.983	(0.977-0.988)	0.998	(0.997-0.999)	0.982	(0.965-0.991)
CCA	0.921	(0.849-0.959)	0.978	(0.956-0.994)	0.921	(0.849-0.959)
Total CA	0.980	(0.973-0.985)	0.996	(0.993-0.998)	0.980	(0.962-0.990)

*, indicates blinded operator. ICC model: two-way mixed, type: absolute agreement. ICC, intraclass correlation coefficient; CI, confidence interval; ICA, internal carotid artery; CCA, common carotid artery; CA, carotid artery.

https://dx.doi.org/10.21037/qims-22-89